

# Comparison of Different Control Concepts for Bearingless Brushless Motors

Franz Zürcher<sup>1,a</sup>, Thomas Nussbaumer<sup>2</sup>, Stefan Walter<sup>1</sup>,  
Christoph Wegmüller<sup>1</sup>, Johann W.Kolar<sup>1</sup>

<sup>1</sup>ETH Zürich, Switzerland

<sup>2</sup>Levitronix GmbH, Switzerland

<sup>a</sup>zuercher@lem.ee.ethz.ch

**Abstract:** Bearingless motors offer various advantages compared to classical motors with mechanical bearings. However, they make great demands on the control algorithms. Due to the availability of very fast low-cost DSP, a lot of new control strategies can be implemented, which offer a lot of different benefits. In this paper, various control algorithms are compared regarding adequate criteria.

**Keywords:** Bearingless Slice Motor, Optimal Control, Robust Control, Control Simulation

## Introduction

In recent years many different bearingless motor concepts(cf.[1] and [2])have been presented, where the radial position of the rotor can be regulated with active magnetic forces during standstill and rotation. They have gained a lot of attractiveness for various applications due to their many advantages such as no friction losses, ultra-high cleanness and compact dimensions. On the other hand, the price of these benefits is an increased effort in the power and control electronics, which are needed for the precise and fast regulation of the rotor position. Typically, the control electronics contain a digital signal processor unit(DSP) which processes the sensor signals, determines the motor state and calculates an optimal output of the bearing power electronics. While in the past the possibilities of low-cost DSPs have been relatively poor, nowadays DSPs with great possibilities including a very highclock-frequency, several integrated analog-to-digital-converters, integrated pulse-width modulation(PWM) generation, preassigned trigonometric functions and a large available internal memory are provided from various companies. These high-end DSPs allow exploring more advanced control algorithms, which have not been possible to implement so far.

In this paper various advanced linear and non-linear control concepts are investigated and compared to a state-of-the-art proportional-integral-differential(PID)controller regarding the disturbance rejection behavior, position control accuracy, position control response time, and the needed processor calculation time. Namely linear PID control, non-linear bang-bang and state-space  $H_\infty$  control are compared regarding adequate criteria. These control concepts are compared by an appropriate mathematical simulation and the most promising ones fulfilling the criteria are implemented and tested on a modern bearingless brushless permanent magnet slice motor as introduced in [3].

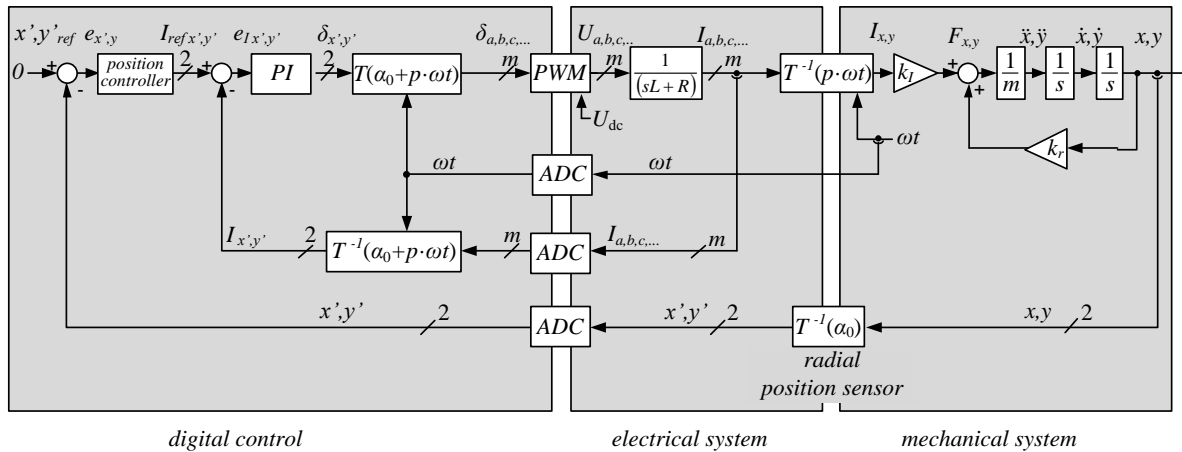


Fig. 1. Radial position control scheme of a multipolar bearingless motor with an inner current control loop and an outer position control loop.

### Control topology

In this paper a magnetic bearing for two degrees of freedom is considered, while the other degrees of freedom are assumed to be stable. This can be achieved by combining two bearingless motor units and an additional thrust bearing as proposed in [4] or alternatively by using an auxiliary passive bearing such as introduced in [5]. The latter concept is called bearingless slice motor and is used for the prototype to verify the calculations in this paper.

The control scheme of the magnetic bearing for the two radial axes  $x$  and  $y$  is depicted in Fig. 1. The whole system can be divided in three parts: the digital control, implemented on a DSP, the electrical system which contains the electrical plant with the ohmic-inductive bearing coils used as electro magnets, and the mechanical system, i.e. the rotor with its inertia force, where the mechanical system can be described by the following equation

$$\begin{bmatrix} \ddot{x} \\ \ddot{y} \end{bmatrix} = \begin{bmatrix} \dot{v}_x \\ \dot{v}_y \end{bmatrix} = \begin{bmatrix} a_x \\ a_y \end{bmatrix} = \frac{1}{m} \left( k_I \cdot \begin{bmatrix} I_x \\ I_y \end{bmatrix} + k_R \cdot \begin{bmatrix} x \\ y \end{bmatrix} \right), \quad (1)$$

where  $m$  is the rotor mass,  $k_I$  the current-force-constant and  $k_R$  the radial stiffness. The interface between the three mentioned system parts is provided by current sensors, position sensors, hall sensors, analog-to-digital-converters (ADC), and a pulse-width modulation element (PWM) to control the bearing currents. The proposed control concept consists of an outer position control loop and an inner current control loop. The rotating transformations  $T(a_0 + p \cdot \omega t)$  and  $T^{-1}(a_0 + p \cdot \omega t)$  are needed for multipolar bearings, where the bearing currents rotate with a frequency  $\omega_{electrical} = p \cdot \omega_{mech}$  and have to be in phase with the air gap flux density distribution. The main control algorithm for the radial position axes  $x$  and  $y$  is in the outer loop and has for all the investigated control algorithms one input and one output per axis (cf. Fig 1, position controller). The input  $e_{x,y}$  is equal to the difference between the reference position  $x_{ref}$  (or  $y_{ref}$ ) and the actual position  $x$  (or  $y$ ). The reference positions  $x_{ref}$  and  $y_{ref}$  are typically set to zero ( $x_{ref} = y_{ref} = 0$ ) to keep the rotor in a center position. The output

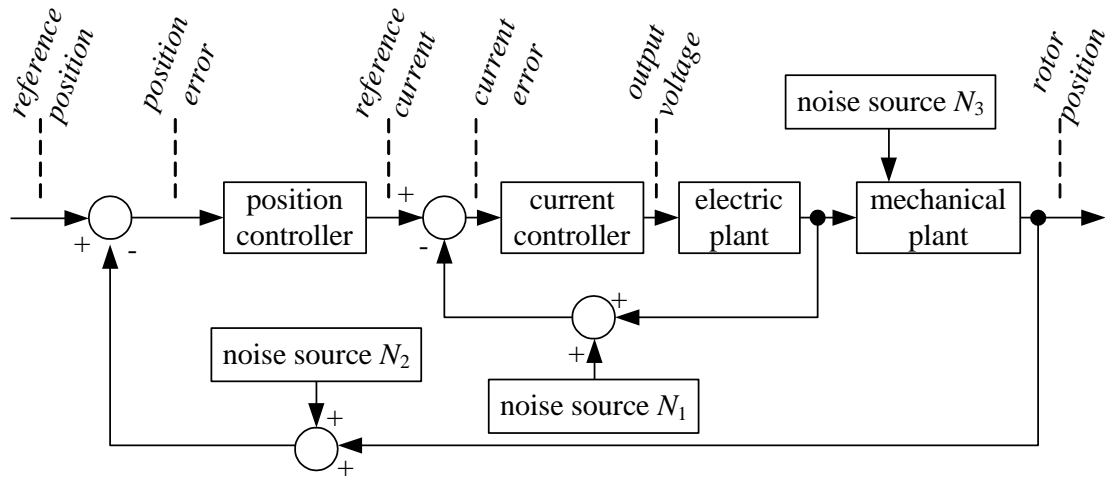


Fig. 2. Abstract mathematical model with the three noise sources  $N_1$ ,  $N_2$  and  $N_3$ .

of the position controller is the reference bearing current  $I_{ref,x}$  (and  $I_{ref,y}$ , respectively) for the inner (current regulating) control loop.

### Mathematical Model

A mathematical model of the system including the plant, the power electronics, the digital signal processor (DSP) software and including various noise sources that simulate sensor noise and a disturbance force acting on the rotor has been developed and implemented with the *Matlab-Simulink* software. Fig. 2 shows a simplified scheme with the three noise sources  $N_1$ ,  $N_2$  and  $N_3$ .  $N_1$  and  $N_2$  simulate sensor noise on the current sensors and position sensors and are modeled as band limited white Gaussian noise, while  $N_3$  simulates a disturbance force acting on the levitated rotor, which is used to model the disturbance rejection behavior of the controller. With the simulation model, the proposed control algorithms can be tested and compared to each other and optimal parameters can be found for each of them without the risk of damaging the hardware prototype. For a fair comparison of the different control algorithms, the optimal parameter set of each of them has to be found by a mathematical derivation. The calculated parameter-sets have been verified by simulation to ensure that there exists no better parameter set for any of the investigated control algorithms.

For the state-space regulators (i.e.  $H_\infty$  and *LQR/LTR*), two state variables per axe have been defined, namely the  $x$  and  $y$  position of the magnetically levitated rotor in  $x$  and  $y$  direction and the velocities  $v_x$  and  $v_y$ . With these four variables it is possible to define the actual system state for every moment  $t$ .

### Control Concepts

Due to the non-linear correlation of the force, bearing current and radial position of the magnetic bearing as well as the limitations of the electrical plant, complex and even non-linear control algorithms can be considered for a stable regulation of the rotor position. There exist a lot of possible control algorithms that can be used to control the rotor position. Each of them features its specific advantages and disadvantages. In this paper, some exemplary control algorithms are chosen and compared to each other. Fig. 3 shows the

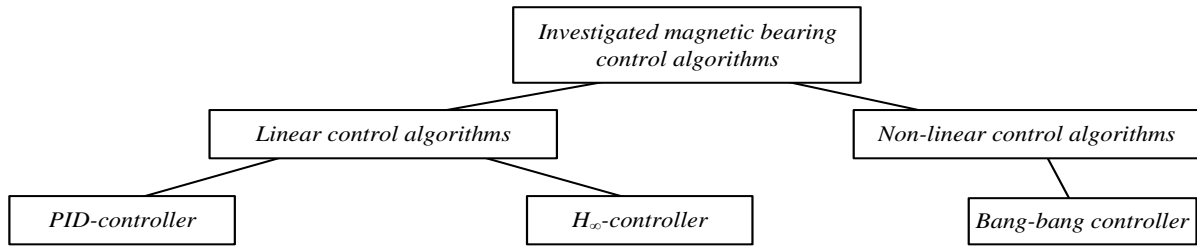


Fig. 3. Classification of the control algorithms, which are investigated in this paper.

classification of some exemplary control algorithms, which are considered to be implemented and tested on the prototype. In the subsequent section these control concepts will be shortly explained.

**PID controller and variations.** Today, many applications of bearingless motors use a state-of-the-art PID linear controller [6] with the three control parameters  $k_P$ ,  $k_I$  and  $k_D$  which regulate the controller output proportional to the position error  $e(t)$ . This leads to the following equation:

$$u(t) = k_P \cdot e(t) + k_I \int_{t_0}^t e(\tau) d\tau + k_D \frac{de(t)}{dt}, \quad (2)$$

which can be rewritten with the Laplace operator as the transfer function

$$K(s) = \frac{u(s)}{e(s)} = k_P + \frac{k_I}{s} + k_D \cdot s. \quad (3)$$

Standard PID are quite fast and easy to implement and achieve good performance results, but they might not be very robust against system nonlinearities as the controller parameters  $k_P$ ,  $k_I$  and  $k_D$  depend strongly on the motor and bearing plant and are typically selected for a specific operating point. In this paper, also variations of the PID controller and combinations with other control algorithms are investigated.

**$H_\infty$  control.** A  $H_\infty$  controller has been presented in [9], [10] and [11], where also a detailed derivation can be found. Therefore, in this paper only a short description is given. The control plant is extended with a virtual input vector  $w$ , which contains the reference position  $x_{ref}$  and with a virtual output vector  $z$ , which contains the output signal  $I_{x,ref}$ . The choice of weighting vectors  $z_e$ ,  $z_u$  and  $z_y$  is the most important task for the design of a stable  $H_\infty$

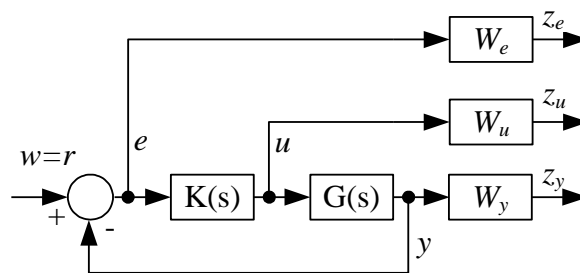


Fig. 4. Expanded control loop for the  $H_\infty$  controller.

controller. The extended plant is depicted in Fig. 4 and the resulting equations are then:

$$\begin{bmatrix} z_e(s) \\ z_u(s) \\ z_y(s) \end{bmatrix} = \begin{bmatrix} W_e(s)S_e(s) \\ W_u(s)K(s)S_e(s) \\ W_y(s)T_e(s) \end{bmatrix} w(s). \quad (4)$$

The control error  $e(s)$  should be minimized and the output signal  $y$  should be equal to the reference position  $r$ . The corresponding  $H_\infty$  problem to solve can be formulated as

$$\|T_{zw}(s)\|_\infty = \left\| \begin{bmatrix} z_e(s)/w(s) \\ z_u(s)/w(s) \\ z_y(s)/w(s) \end{bmatrix} \right\|_\infty = \left\| \begin{bmatrix} W_e(s)S(s) \\ W_u(s)K(s)S(s) \\ W_y(s)T(s) \end{bmatrix} \right\|_\infty \leq 1, \quad (5)$$

where  $\|T_{zw}(s)\|$  corresponds to the  $H_\infty$  norm of the transfer function  $T_{zw}$  of the expanded system. The  $H_\infty$  norm is defined as the maximum singular value of the function  $T_{zw}(s)$ :

$$\bar{\sigma} = \sqrt{\lambda_{\max}\{T_{zw}^H T_{zw}\}}. \quad (6)$$

More information about  $H_\infty$  control can be found in [9], [10] and [11]. Also a linear quadratic Gaussian controller with loop transfer recovery (LQR/LTR,) (cf. [12]) has been considered and some simulations have been done. The advantage of LQR/LTR control is that sensor noise can be integrated in the mathematical model. The expected results do not differ much from those of the  $H_\infty$  control. Therefore only the  $H_\infty$  control has been considered as a state-space controller to implement on the prototype.

**Bang-bang controller.** A controller with exactly two possible output states is called bang-bang controller. This is the simplest possible non-linear controller. As shown in Fig. 5 (a) a simple relay switches between the two output states  $+I_{max}$  and  $-I_{max}$ , depending on the sign of the position error  $e$ :

$$\begin{bmatrix} I_{x \text{ out}} \\ I_{y \text{ out}} \end{bmatrix} = \begin{cases} +I_{\max} & \text{if } e_{x,y} \geq 0 \\ -I_{\max} & \text{if } e_{x,y} < 0 \end{cases}. \quad (7)$$

A pure bang-bang cannot stabilize the position of the magnetic bearing plant. Fig. 6 (a) shows the unstable behaviour of one radial position axis of the magnetic bearing without a controller by state diagram analysis, whereby the system state variable position change velocity  $v_x = dx/dt$  (and  $v_y = dy/dt$ , respectively) is plotted against the position  $x$  (and  $y$ , respectively). Adding a bang-bang controller results in the trajectories depicted in Fig. 6 (b).

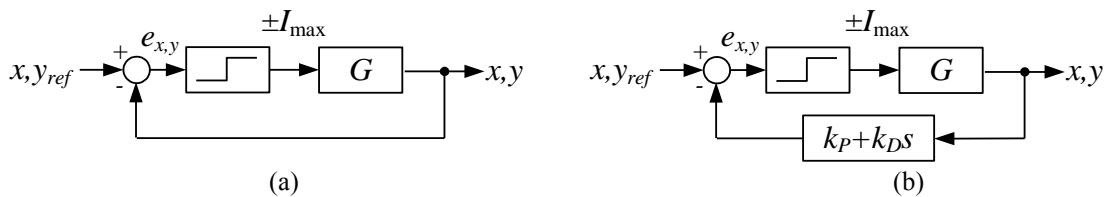


Fig. 5. Simplified control loop of the pure bang-bang controller (a) and the bang-bang controller with an additional damping element in the feedback-loop.

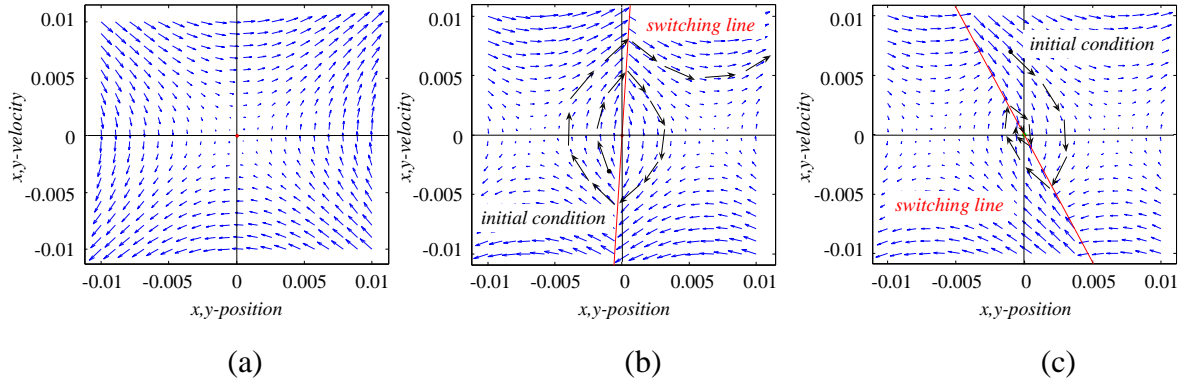


Fig. 6. State diagram of the unstable system without controller (a), unstable system with a pure bang-bang controller and the stabilized system with a bang-bang controller with an additional damping element.

As one can see, the plant is still unstable for all trajectories, because the switching line  $x, y = 0$  gets slightly tilted due to the delay caused by the parasitic lowpass filter of the sensor and, therefore, the system gets destabilized. But the system can be stabilized by adding an additional derivative part to the feedback path of the measured positions  $x$  and  $y$ :

$$\begin{bmatrix} I_{x \text{ out}} \\ I_{y \text{ out}} \end{bmatrix} = \begin{cases} +I_{\max} & \text{if } -k_p \begin{bmatrix} x \\ y \end{bmatrix} - k_D \begin{bmatrix} v_x \\ v_y \end{bmatrix} + \begin{bmatrix} x_{ref} \\ y_{ref} \end{bmatrix} \geq 0 \\ -I_{\max} & \text{if } -k_p \begin{bmatrix} x \\ y \end{bmatrix} - k_D \begin{bmatrix} v_x \\ v_y \end{bmatrix} + \begin{bmatrix} x_{ref} \\ y_{ref} \end{bmatrix} < 0 \end{cases} \quad (8)$$

The bang-bang controller expanded in this manner is depicted in Fig. 5 (b). Equation (8) together with the differential equation of the mechanical system (1) gives the following solution of the differential equation in  $x$ -direction:

$$v_x = \dot{x} = \sqrt{\frac{k_S}{m} x^2 + \frac{2k_i I_{\max} \text{sign}(-k_p x - k_D v_x + x_{ref})}{m}} \quad (9)$$

This results in a stable system, as shown in Fig. 6 (c) due to the negative slope of the switching line which is rotated in counter-clockwise direction due to the derivative part  $k_D$  in the feedback path.

## Results and experimental verification

Based on the introduced model (cf. Fig. 2) the different control algorithms have been

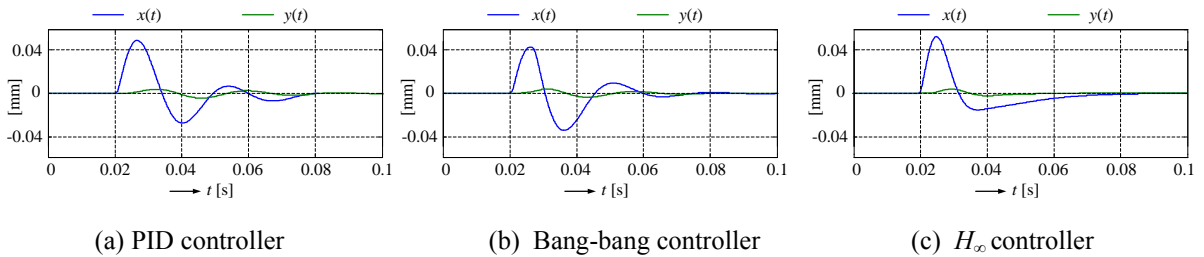


Fig. 7. Simulated disturbance response of the PID controller (a), the bang-bang controller with an additional damping element (b), and the  $H_\infty$  controller (c) and a disturbance force  $F_x = 50$  N during 1.1 ms.

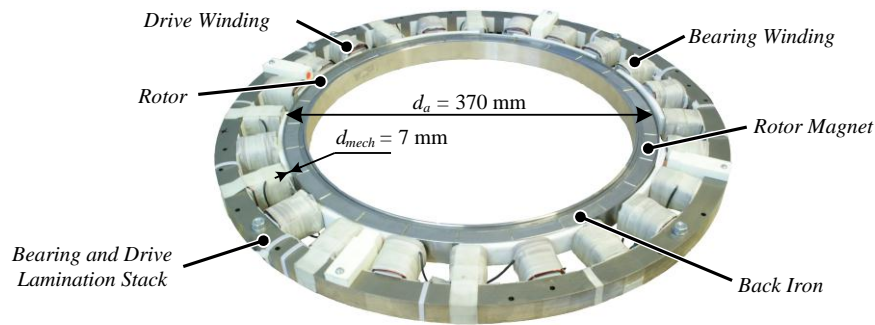


Fig. 8. Photo of the bearingless fractional slot motor (cf. [5]) prototype which was used to compare the different control algorithms.

simulated and analyzed regarding the aforementioned criteria to choose the most optimal algorithm. Fig. 7 shows exemplarily the simulated response to an axial disturbance force  $F_z$  applied for a defined period of time  $t_d$  for three different controller types, namely the  $PID$  controller, a bang-bang controller with an additional damping element and a  $H_\infty$  controller. Interestingly, the three control methods exhibit similar dynamic performance, whereby the  $H_\infty$  controller shows the fastest reaction and smallest error integral.

To verify the simulation results the control algorithms have been implemented on a

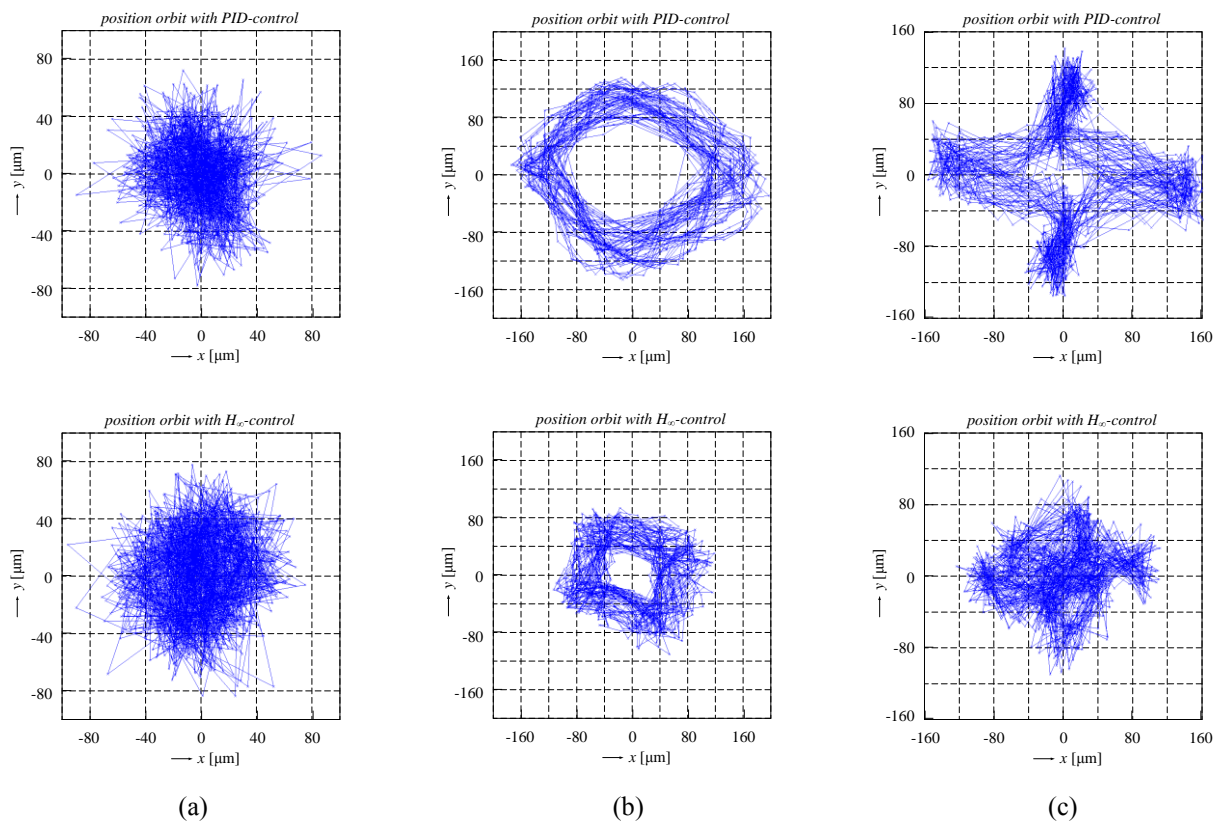


Fig. 9. Position orbit  $x,y(t)$  of the magnetically levitated rotor during rotation at  $n_{\max} = 1500$  r/min (a), rotation at the critical mechanical resonance speed  $n_{\text{resonance}} = 72$  r/min (b) and rotation at  $n = 500$  r/min with a strong mass-unbalance.

Table 1

Qualitative comparison of the different control algorithms, where (+) is an especially good performance, (✓) is an average performance and (-) is a rather weak performance in the respective category.

	PID controller	Bang-bang controller with damping	$H_\infty$ controller
Real-time computation time	✓	+	-
Control speed	✓	✓	+
Implementation effort	✓	+	-
Robustness	✓	-	+
Number of parameters	-	+	-
Intuitive understanding	✓	+	✓

bearingless fractional slot motor which was introduced in [5] (cf. Fig. 8) and compared according to the aforementioned criteria. In particular, the two most promising control algorithms due to the simulation results, namely the *PID controller* and  *$H_\infty$  controller* have been compared under different conditions. Fig. 9 shows exemplarily the position orbit of the levitated rotor at a rotational speed of  $n = 1500$  r/min in (cf. Fig. 9 (a)), at the critical mechanical resonance speed  $n_{res} = 72$  r/min (cf. Fig. 9 (b) and at a speed of  $n = 500$  r/min with a strong mass unbalance fixed on the rotor (cf. Fig. 9 (c)). As one can see the robust  $H_\infty$  controller copes much better with the extreme conditions mass-unbalance and mechanical resonance speed.

### Experimental comparison of the control algorithms

In Table 1 the different control algorithms are compared regarding different criteria. One can see that no control method is superior in all aspects. The  $H_\infty$  controller for example is very robust against external disturbances but needs a considerable implementation effort. The very simple bang-bang controller on the other hand cannot stabilize the system without additional measures. The conventional PID control might be a good compromise between control performance and implementation effort in many cases. In any case, for each particular application the control algorithm has to be chosen carefully in dependency on the specific demands. The investigations of this paper might help to select the appropriate controller, if the desired control conditions and requirements are known.

### Summary

In this paper, a simulation model of a magnetically levitated motor system and corresponding power electronics has been developed and several different control algorithms have been tested. The most promising ones based on the simulation results have been



implemented on a DSP, namely a PID controller and a  $H_\infty$  controller. Especially under extreme conditions like rotating with a mass-unbalance or rotating at the critical mechanical resonance speed the  $H_\infty$  controller behaves significantly better, but is characterized by a large implementation effort.

## References

- [1] Salazar,A.Chiba,T.Fukao,“A review of development in bearingless motors,” 7th Int.Symp.on Magn.Bearings,Zurich,Switzerland,Aug.23-25,2000,pp.335-340.
- [2] P.Karutz,T.Nussbaumer,J.W.Kolar,“Magnetically levitated slice motors-an overview,”Energy Conversion Congress and Exposition 2009,IEEE ECCE 2009, vol.,no.,pp.1494-1501,20-24 Sept.2009
- [3] R.Schoeb and N.Barletta,“Principle and application of a bearingless slice motor,”JSME Int.J.Series C,vol.40,pp.593–598,1997.
- [4] Q.Hijikata,S.Kobayashi,M.Takemoto,Y.Tanaka,A.Chiba,and T.Fukao, “Basic characteristics of an active thrust magnetic bearing with a cylindrical rotor core,”IEEE Transactions on Magnetics.,vol.44,no.12,pp.4167–4170,Dec.2008.
- [5] F.Zürcher F,T.Nussbaumer,W.Gruber,J.W.Kolar,“Design and Development of a 26-Pole and 24-Slot Bearingless Motor,”IEEE Transactions on Magnetics Volume 45,Issue 10,2009,pp.4594-4597.
- [6] A.Kiam Heong,G.Chong,Yun Li,“PID control system analysis,design,and technology,”IEEE Transactions on Control Systems Technology,vol.13,no.4,pp.559-576,July 2005.
- [7] G.F.Franklin,J.D.Powell,A.Emami-Naeini,“Feedback Control of Dynamic Systems,”5th Edition,New Jersey:Pearson Prentice Hall,2006,ISBN 0–13–149930–0.
- [8] S.Skogestad,I.Postlethwaite,“Multivariable Feedback Control,Analysis and Design,”Reprinted February 2007,Chichester:John Wiley&Sons,1996,ISBN0–470–01168–8.
- [9] U.Christen,H.P.Geering, “ Inverting and noninverting  $H_\infty$  controllers,”Systems&Control Letters,30(1997),pp.31-38.
- [10] U.Christen,M.F.Weilenmann,H.P.Geering,H.P,“Design of  $H_2$  and  $H_\infty$  controllers with two degrees of freedom,”American Control Conference 1994,vol.3,no.,pp.2391-2395 vol.3,29 June-1 July 1994.
- [11] U.Christen, “Engineering Aspects of  $H_\infty$  Control,” ETH Zürich,Diss.,1996. – Nr.11433.
- [12] H.P.Geering,“Robuste Regelung,”lecture script,ETH Zürich,May 2007